

Preliminary Results of Discrimination Studies in Western China

Hans E. Hartse, Steven R. Taylor, and George E. Randall
Geophysics Group - EES-3, Los Alamos National Lab

Sponsored by U.S. Department of Energy

ABSTRACT

As a part of the Comprehensive Test Ban Treaty Research and Development Program, we have started to evaluate regional seismic discriminants for western China. Our primary objective is to appraise the current seismic discrimination capability for central and south-central Asia. We have been testing several discriminants using short-period and broadband waveforms recorded at the Chinese Digital Seismic Network station WMQ. Our preliminary results cover four classes of discriminants: (1) short-period ratios, (2) short-period spectral ratios, (3) long-period ratios, and (4) long-period to short-period ratios. For each discriminant tested, we have measured waveforms from over 140 earthquakes to find ratio-distance relationships, and we have used these relationships to correct our final ratio- m_b discrimination plots for distance effects.

To date, we have evaluated earthquakes that range in magnitude (m_b) between 3.8 and 6.2 and occurred up to 1200 km from WMQ. We have evaluated about 15 underground nuclear explosions from the Kazakh test site ($4.5 < m_b < 6.1$ and $\Delta \approx 960$ km) and a single nuclear explosion from the Lop Nor test site ($m_b = 4.6$ and $\Delta = 260$ km). For this range of magnitudes and distances, we find that most of the discriminants outlined above (with the exception of the spectral discriminant) separate the explosion and earthquake populations. We find that the absence of a Love wave accompanied by the presence of a Rayleigh wave is a strong indicator of an explosion. Such an occurrence is apparently rare for central Asian earthquakes. We plan to continue this study by, processing other regional data, developing regional m_b , M_s , and coda magnitude scales, and testing the m_b / M_s and coda discriminants. We will be applying multivariate techniques to combine discriminants and assess discrimination capabilities.

OBJECTIVE

As a part of the Comprehensive Test Ban Treaty (CTBT) Research and Development Program, we have started to evaluate regional seismic discriminants for western China. Our primary objective is to appraise the current seismic discrimination capability for central and south-central Asia. We have been testing several known discriminants (*cf. Pomeroy et al., 1982; Taylor et al., 1989*) using waveforms recorded with the Chinese Digital Seismic Network (CDSN). Here we present results for station WMQ in northwest China. These preliminary results cover four classes of discriminants: (1) short-period ratios (such as P_g / L_g), (2) short-period spectral ratios (such as $L_g (1-2 \text{ Hz}) / L_g (6-8 \text{ Hz})$), (3) long-period ratios (Love wave (L) / Rayleigh wave (R)), and (4) long-period to short-period ratios (such as L / P_g). We compute distance corrections by linear regression of earthquake ratios on the logarithm of distance and apply the corrections to both earthquake and explosion ratios. To date, we have analyzed about 140 earthquakes that range in magnitude (m_b) between 3.8 and 6.2 and range in epicentral distance between about 100 and 1200 km. We have evaluated about 15 underground nuclear explosions from the Kazakh test site (KTS) and a single nuclear explosion from the Lop Nor test site. The explosions range in magnitude between 4.6 and 6.1 and range in epicentral distance between about 260 and 980 km. For this range of magnitudes and distances, we find that most of the discriminants outlined above (with the exception of the spectral discriminant) separate the explosion and earthquake populations.

RESEARCH ACCOMPLISHED

Waveforms obtained. Our data source for this project has been the IRIS Data Management Center (DMC). Using NEIC/ISC event catalogs maintained at the IRIS DMC, we have requested and obtained short-period (SH, 40 sps) and broadband (BH, 20 sps) waveforms from about 140 earthquakes and 16 nuclear explosions recorded at station WMQ. The locations of these events, along with station locations and some geographic features, are shown in Figure 1. We obtained and processed data from events shown in the box surrounding station WMQ. Waveforms of a single explosion from Lop Nor are available through IRIS. This explosion is about 260 km from WMQ and has a reported m_b of 4.6. About 15 nuclear explosions from KTS have been recorded at WMQ. The KTS explosions are between about 950 and 980 km from WMQ. Magnitudes of these explosions range between 4.6 and 6.1. Most earthquakes composing our data set occurred to the south, southwest, and west of WMQ. They range in magnitude between 3.8 and 6.2. Maximum epicentral distance for the earthquakes is about 1200 km.

Waveforms and Processing - Short Periods. To evaluate short-period discriminants, we measured bandpass filtered velocity records for P_n , P_g , S_n , and L_g rms amplitudes. Prior to measuring phase amplitudes, we handpicked the clearest arrivals for each phase on unfiltered, three-component records, and measured velocities for each phase. Using the velocities of each phase, we defined group velocity windows centered on each phase, and then automatically measured rms amplitudes within the windows. The centers of the frequency bands evaluated range between 1 and 9 Hz.

An earthquake from January, 1990 has nearly the same epicenter and m_b as the Lop Nor explosion (Figure 1). As an example of our data processing procedure, we compare short-period records of this explosion and earthquake in Figure 2. Each event shows the unfiltered SHZ velocity record and two bandpass filtered waveforms. Also shown are the P_g and L_g measurement windows. P_n and S_n were not measured on these records because the event-station distance is too short for a clear head wave arrival from the crust-mantle boundary. Note that for the 1-2 Hz band the P_g and L_g amplitudes of the explosion are about the same. However, for the 4-8 Hz band, the P_g amplitude is much greater than the L_g amplitude. For the earthquake, the L_g amplitude is always greater than the P_g amplitude.

Waveforms and Processing - Long Periods. Figure 3 shows Rayleigh waves and Love waves from the same explosion and earthquake discussed above. Here, we show broadband

displacement records filtered between 8 and 16 seconds. By visually inspecting many long-period records, we selected L and R group velocities that allowed us to automatically pick peak-to-peak maximum amplitudes for each surface wave phase. We also processed surface waves for 6-12 s, 12-24 s, and 16-32 s periods. L and R from the earthquake have about the same maximum amplitudes, while R for the explosions is about four times greater than L . Indeed, L from the explosion source is such a weak, poorly developed phase, that it often barely exceeds noise levels. Although these events have the same m_b , the amplitudes of the earthquake surface waves are more than a factor of 10 greater than the amplitudes of the explosion surface waves.

Short-Period Discriminants. Many short-period regional discriminants that exploit a P/S ratio have been discussed in the literature (cf. *Pomeroy et al.*, 1982). Figure 4 shows two of our examples from China. For each discriminant, we show the ratio-distance trend obtained from earthquake data, and we present a ratio- m_b discrimination plot where all have been corrected for distance. All ratios shown have signal that is at least 2.5 times the measured noise level. The 1-2 Hz P_g/L_g ratio does not separate the explosion and earthquake populations nearly as well as the 4-8 Hz ratio. We find that for frequency bands above 3 Hz, the populations can be separated for P_g/L_g , P_n/L_g , and P_n/S_n ratios. However, considering signal-to-noise ratios of these four body wave phases, we find that the P_g/L_g ratio is most useful.

Short-Period Spectral Discriminants. Spectral discriminants have been successfully applied to relatively small events from the western United States. *Taylor et al.* (1988) used the $L_g(1-2\text{ Hz}) / L_g(6-8\text{ Hz})$ ratio, *Bennett and Murphy* (1986) used the $L_g(0.5-1\text{ Hz}) / L_g(2-4\text{ Hz})$ ratio, and *Hartse et al.* (1995) used the coda $(0.5-1\text{ Hz}) / (2-4\text{ Hz})$ ratio to separate nuclear explosions from earthquakes. However, Figure 5 shows that the spectral discriminant for western China may not be as successful. The $L_g(1-2\text{ Hz}) / L_g(6-8\text{ Hz})$ ratio fails to separate the events. We also have tried $L_g(0.5-1\text{ Hz}) / L_g(2-4\text{ Hz})$ ratios and various P_g/L_g spectral ratios with results similar to those in Figure 5. The western U.S. studies generally examined small explosions ($m_b < 4.8$) that were detonated above the water table. Most explosions from Asia are thought to be detonated below the water table (*Matzko*, 1994). As discussed by *Taylor and Denny* (1991), the amount of gas-filled porosity near the explosion appears to control the performance of the spectral-ratio discriminant.

Long-Period Discriminants. We tested long-period L/R discriminants in four frequency bands, and found that the 8-16 s period shows the best separation and least scatter (Figure 6). The L/R discriminant was mentioned by *Pomeroy et al.* (1982), but has not been widely applied. The problem is that the weak L of the explosions often fail to exceed noise levels. The Kazakh explosions had to be large ($m_b > 5.5$) to generate L that was above the noise at WMQ, over 950 km from the station. However, for smaller events, the absence of L combined with the presence of R can be used as an explosion indicator. We measured L and R of over 100 earthquakes and found only four events (<4%) where L was below the noise while R was above the noise. At the same time, of the 15 Kazakh explosions we processed, we found four (>25%) with L below the noise and R above the noise.

Short-Period/Long-Period Discriminants. We tested P_g/L and P_g/R ratios. These discriminants are analogous to the m_b/M_s discriminant that has been successfully applied in the western U.S. (*Taylor et al.*, 1989). Because we have not yet developed regional m_b and M_s scales for station WMQ, we have simply tested $P_g /$ surface wave ratios. We measured peak-to-peak displacement amplitudes from broadband records to test this discriminant. Figure 7 shows the $P_g(2-4\text{ Hz}) / L(8-16\text{ s})$ and the $P_g(2-4\text{ Hz}) / R(8-16\text{ s})$ ratios versus m_b . We also tested $P_g(1-2\text{ Hz})$, but found that $P_g(2-4\text{ Hz})$ produces better separation. L performs better than R , but, as in the case of the long-period discriminants, L for smaller explosions is difficult to measure above the noise.

RECOMMENDATIONS AND FUTURE PLANS

We have started a comprehensive seismic discrimination study of western China. Using waveforms from over 100 earthquakes and 16 nuclear explosions recorded at CDSN station WMQ, we have tested short-period phase ratios, short-period spectral ratios, long-period ratios, and short-period/long-period ratios as event discriminants. We have estimated and applied distance corrections for every discriminant tested. We find that the absence of a Love wave accompanied by the presence of a Rayleigh wave is a strong indicator of an explosion. This appears to be a rare occurrence for central Asian earthquakes. With the exceptions of the short-period spectral ratio, we have been able to separate earthquakes from underground nuclear explosions for events down to $m_b \approx 4.5$ at distances of about 1000 km. However, we have not yet processed any chemical explosion data. We do not know what our discrimination capabilities will be for smaller explosions.

Our study has progressed to where the performance of some discriminants can be compared between the western China region and the western U.S. In Figure 8 we compare event separation for these two regions using the P_g/L_g ratio. The figure shows average ratios and one standard deviation for earthquakes and nuclear explosions plotted against frequency. Compared to the U.S., in western China, separation is greater and occurs at lower frequencies. As more events are processed from Asia, the separation may decrease. However, the good separation at about 3 Hz implies that this regional discriminant can be applied at greater distances in central Asia than in the western U.S. Additionally, the scatter of the P_g/L_g ratio appears to be less for western China than for the western U.S. at higher frequencies.

Future work will involve expanding outward from western China. We have obtained, but have not yet processed, waveforms recorded at stations AAK and TLY (Figure 1), and we will obtain and process other regional data. We will develop regional m_b , M_s , and coda magnitude scales, and test the m_b/M_s and coda discriminants. Because we have tested several different discriminants, we have been preparing multivariate techniques that combine discriminants and discrimination capabilities. We will analyze smaller magnitude events by acquiring Chinese provincial catalogs and obtaining these events from the IRIS DMC.

REFERENCES

- Bennett, T., and J. Murphy, Analysis of seismic discrimination using regional data from western United States events, *Bull. Seis. Soc. Am.*, 76, 1069-1086, 1986.
- Hartse, H. E., W. S. Phillips, M. C. Fehler, and L. S. House, Single-station spectral discrimination using coda waves, *Bull. Seis. Soc. Am.*, 85, in-press, 1995.
- Matzko, J. R., Geology of the Chinese nuclear test site near Lop Nor, Xinjiang Uygur Autonomous Region, China, *Engineering Geology*, 36, 173-181, 1994.
- Pomeroy, P. W., J. B. Best, and T. V. McEvelly, Test ban treaty verification with regional data - a review, *Bull. Seis. Soc. Am.*, 72, S89-S129, 1982.
- Taylor, S. R., N. W. Sherman, and D. D. Marvin, Spectral discrimination between NTS explosions and western United States earthquakes at regional distances, *Bull. Seis. Soc. Am.*, 78, 1563-1579, 1988.
- Taylor, S. R., M. D. Denny, E. S. Vergino, and R. E. Glaser, Regional discrimination between NTS explosions and western U.S. earthquakes, *Bull. Seis. Soc. Am.*, 79, 1142-1176, 1989.
- Taylor, S. R., and M. D. Denny, An analysis of spectral differences between Nevada Test Site and Shagan River nuclear explosions, *J. Geophys. Res.*, 96, 6237-6245, 1991.

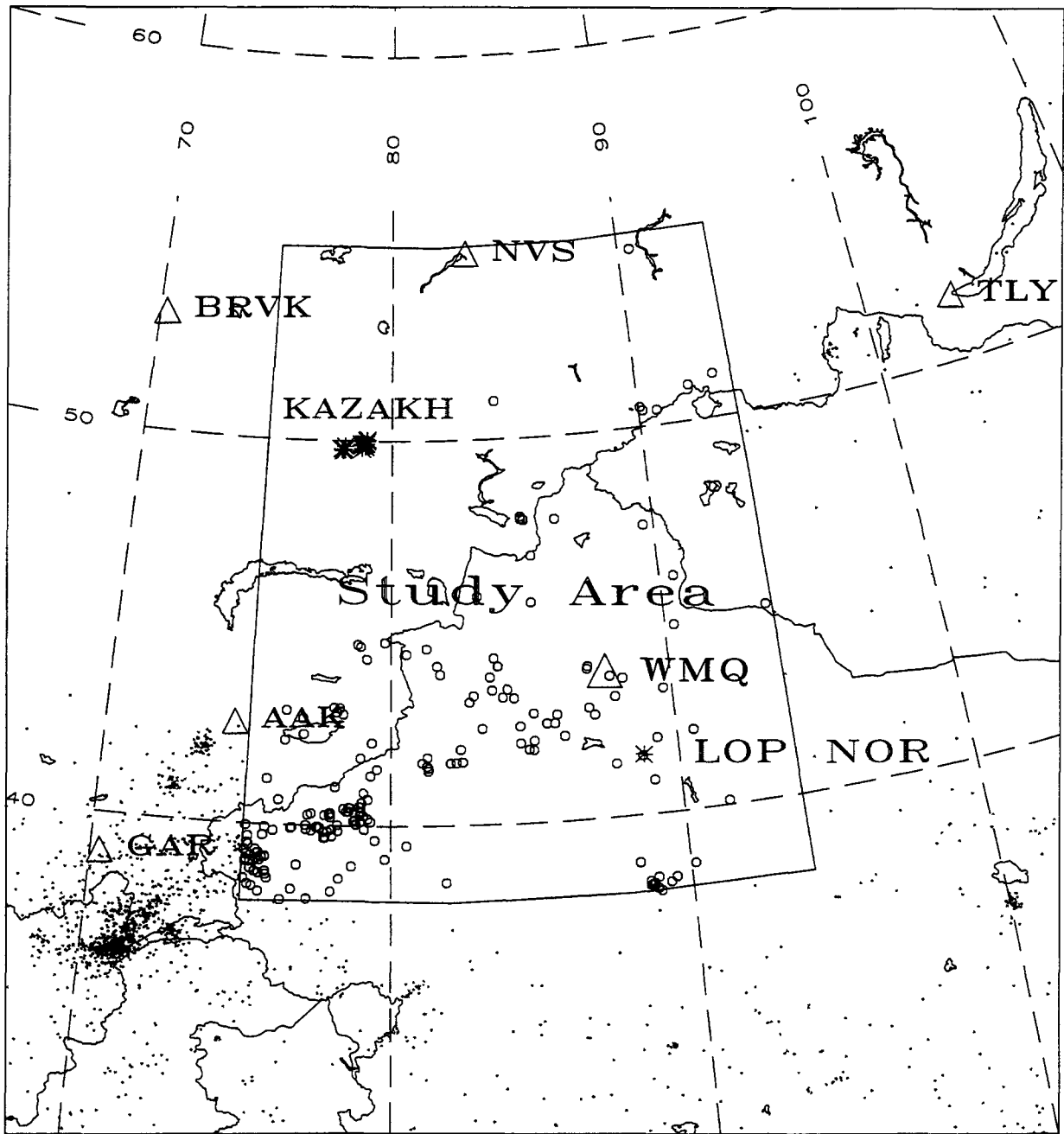


Figure 1. Event location map of central Asia for the years 1989-1994. Large symbols inside study area box denote events for which we have obtained and processed waveforms. Asterisks denote nuclear explosions and circles denote earthquakes. Small dots outside study area represent earthquakes that we have not investigated. For scale, it is about 260 km from Lop Nor to station WMQ and about 970 km from the Kazakh test site to station WMQ. Locations are from the National Earthquake Information Center catalogs maintained at the IRIS Data Management Center.

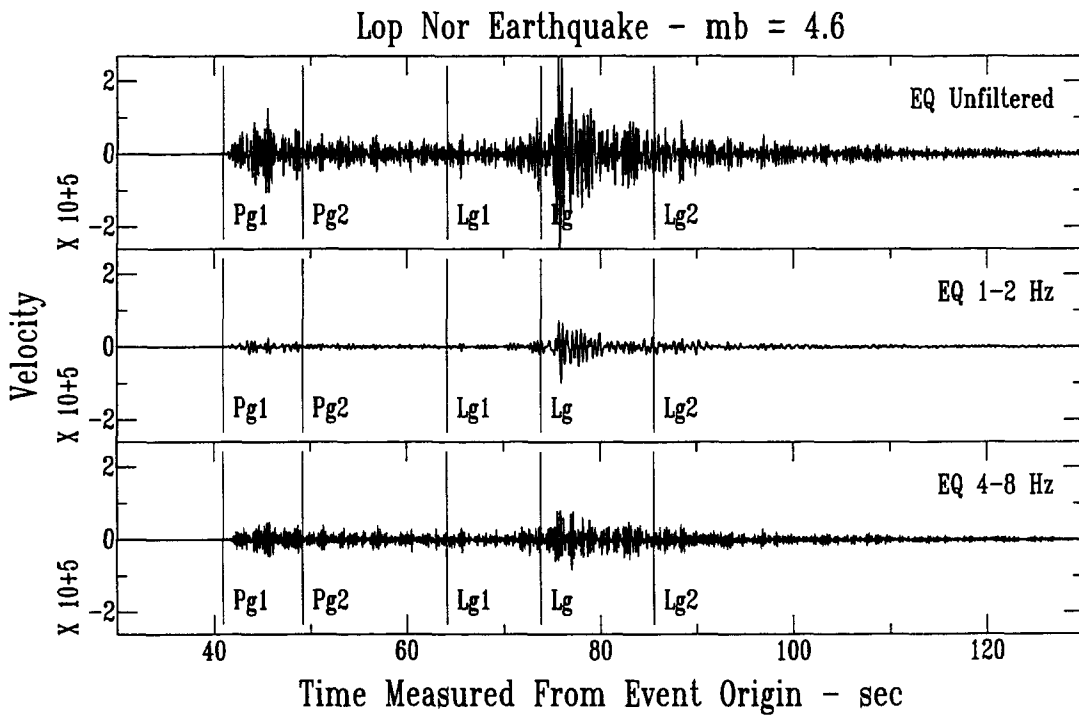
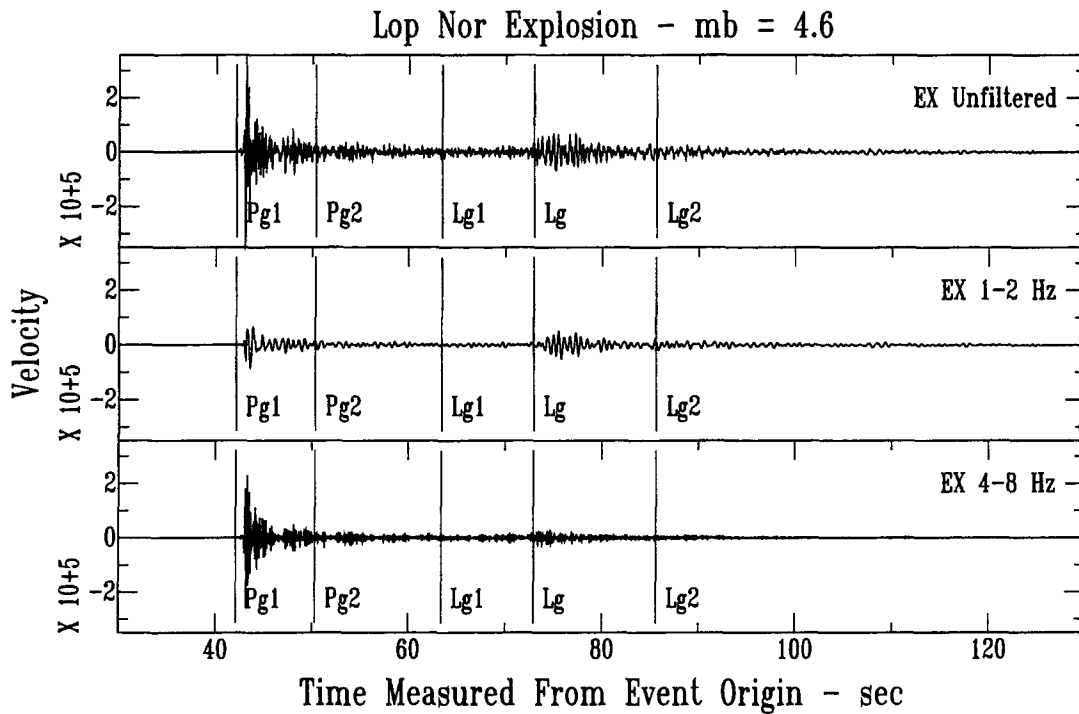


Figure 2. Short-period, vertical component (SHZ) waveforms recorded at station WMQ for the September 29, 1988 Lop Nor nuclear explosion (*top*) and a nearby earthquake from 1990 (*bottom*) (see Figure 1 for locations). Unfiltered, bandpass filtered from 1-2 Hz, and bandpass filtered from 4-8 Hz waveforms are displayed in velocity. P_g and L_g measurement windows are marked by Pg1, Pg2, Lg1, and Lg2. For both events, $m_b \approx 4.6$ and event-station distance is about 260 km. Note the strong P_g phase of the explosions and that the P_g / L_g ratio of the explosion increases as passbands are increased to above 4 Hz.

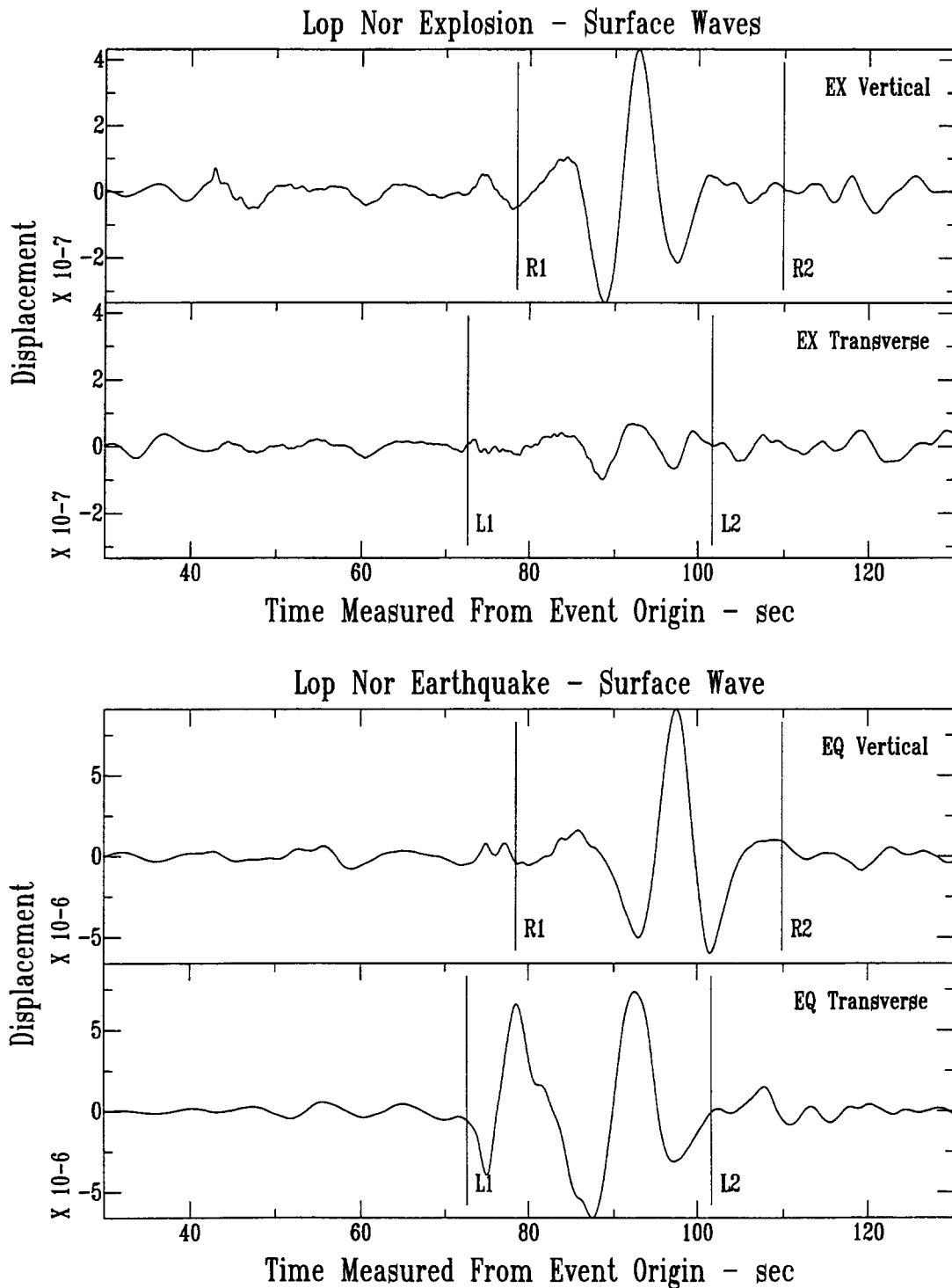


Figure 3. Long-period (8-16 s) surface waves recorded with broadband seismometers at station WMQ. These are the same events shown in Figure 2, but the long periods are displayed in displacement. *Top* shows the explosion Rayleigh wave between R1 and R2 markers and the Love wave between L1 and L2 markers. *Bottom* shows the Rayleigh and Love wave of the earthquake. Note that the Love wave for the explosion is extremely weak relative to the Rayleigh wave, while the Love and Rayleigh wave of the earthquake have comparable amplitudes. Also, despite the similar magnitudes (≈ 4.6), the surface waves of the explosion are much weaker than those of the earthquake.

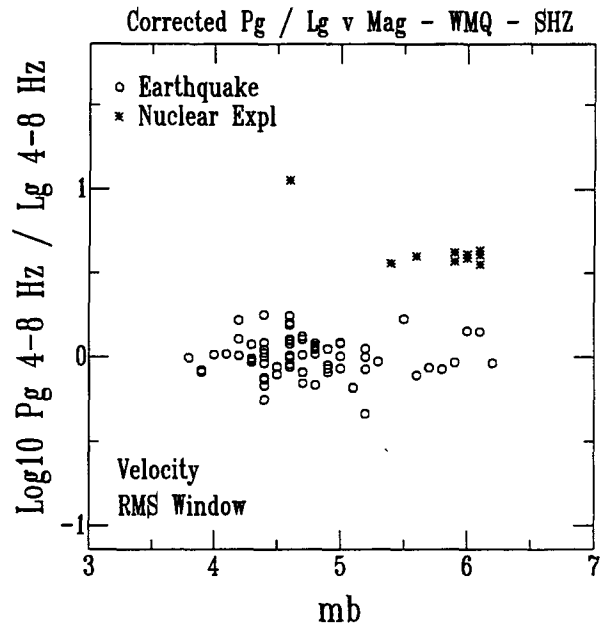
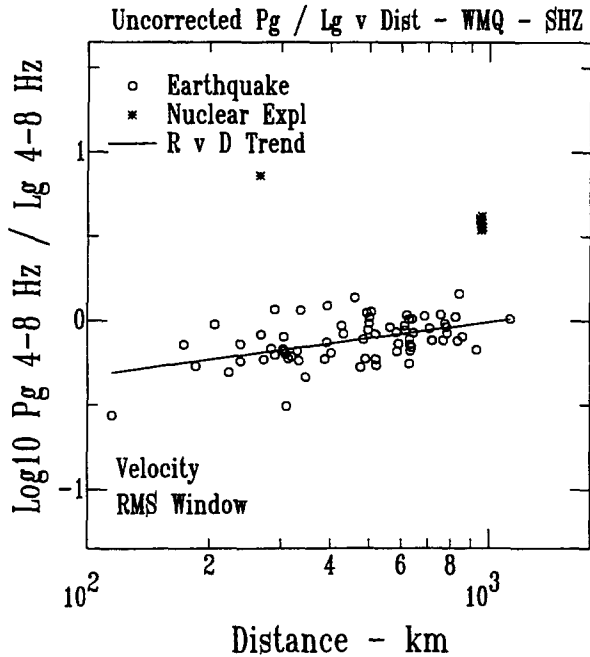
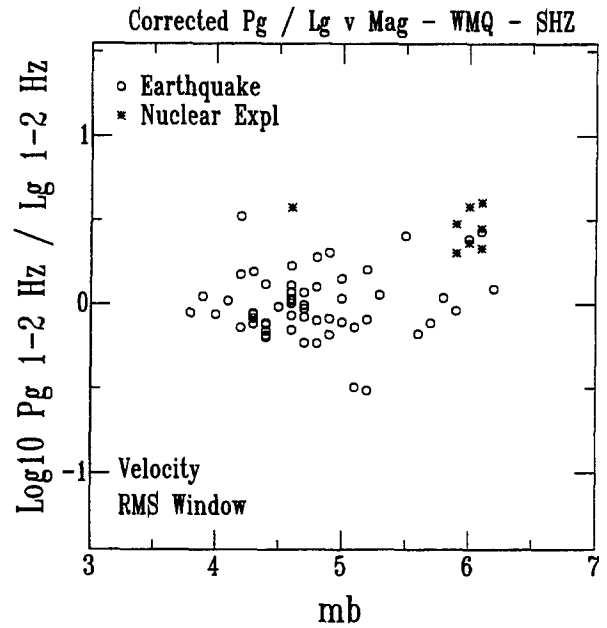
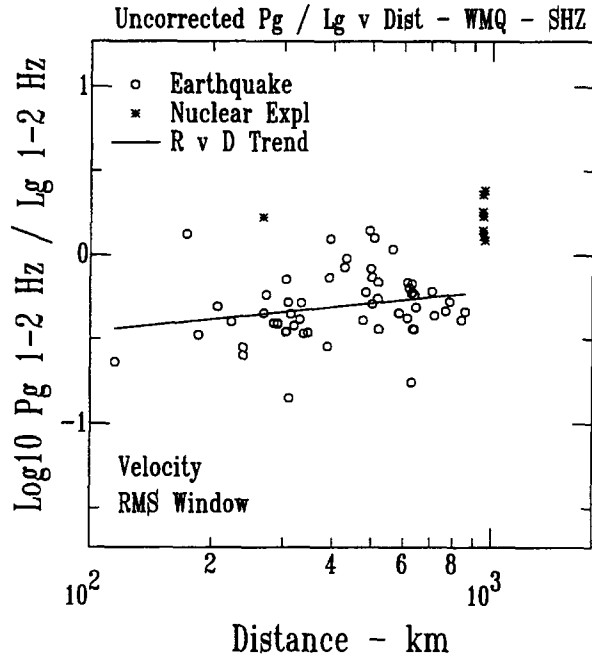


Figure 4. Short-period discrimination plots for station WMQ. *Top* shows $P_g(1-2\text{ Hz})/L_g(1-2\text{ Hz})$ results, and *bottom* shows $P_g(4-8\text{ Hz})/L_g(4-8\text{ Hz})$ results. Ratio-distance trend (slope and intercept) is obtained from the earthquake measurements, and trend is removed in the ratio-magnitude discrimination plots (on *right*). Waveform rms amplitudes are measured from short-period, vertical component (SHZ) velocity records. Note increased separation between earthquakes and explosions as frequency increases.

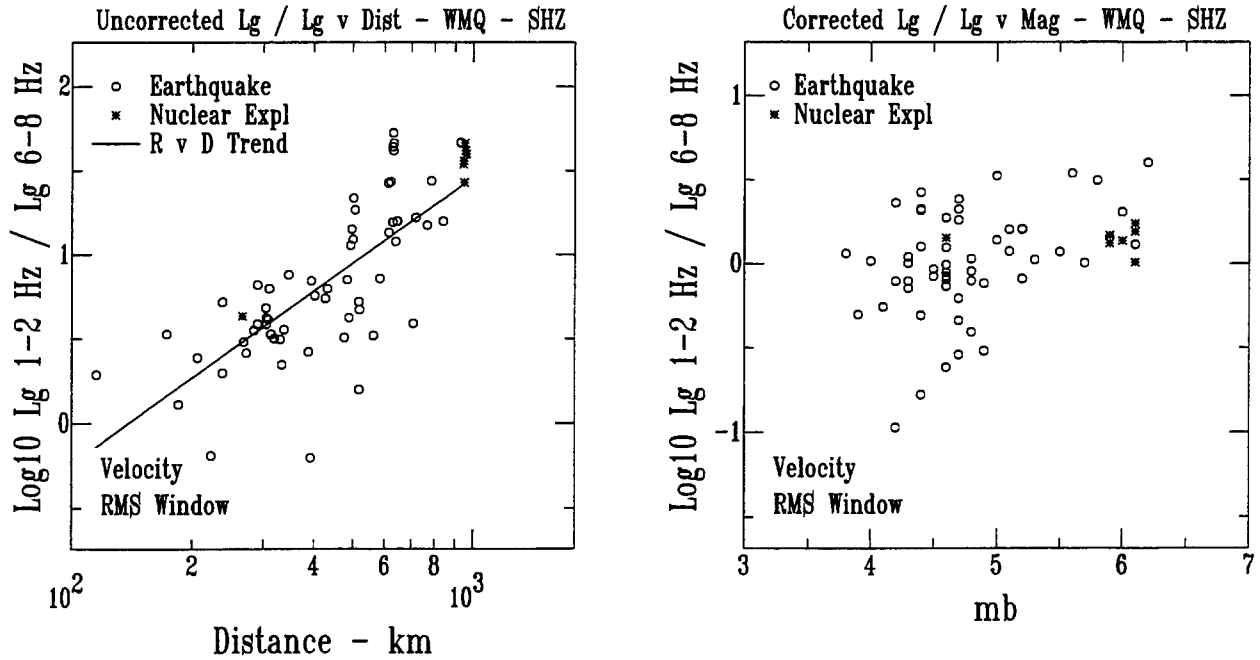


Figure 5. Short-period spectral discrimination plots for station WMQ. The $L_g(1-2)/L_g(6-8)$ spectral discriminant was successfully applied to events from the western U.S. by Taylor *et al.* (1988), but, for south-central Asia, the $L_g(1-2)/L_g(6-8)$ spectral ratio apparently does not perform well. Distance corrections have been applied to the ratio-magnitude plot as described in Figure 4. Waveform rms amplitudes are measured from short-period, vertical-component (SHZ) velocity records.

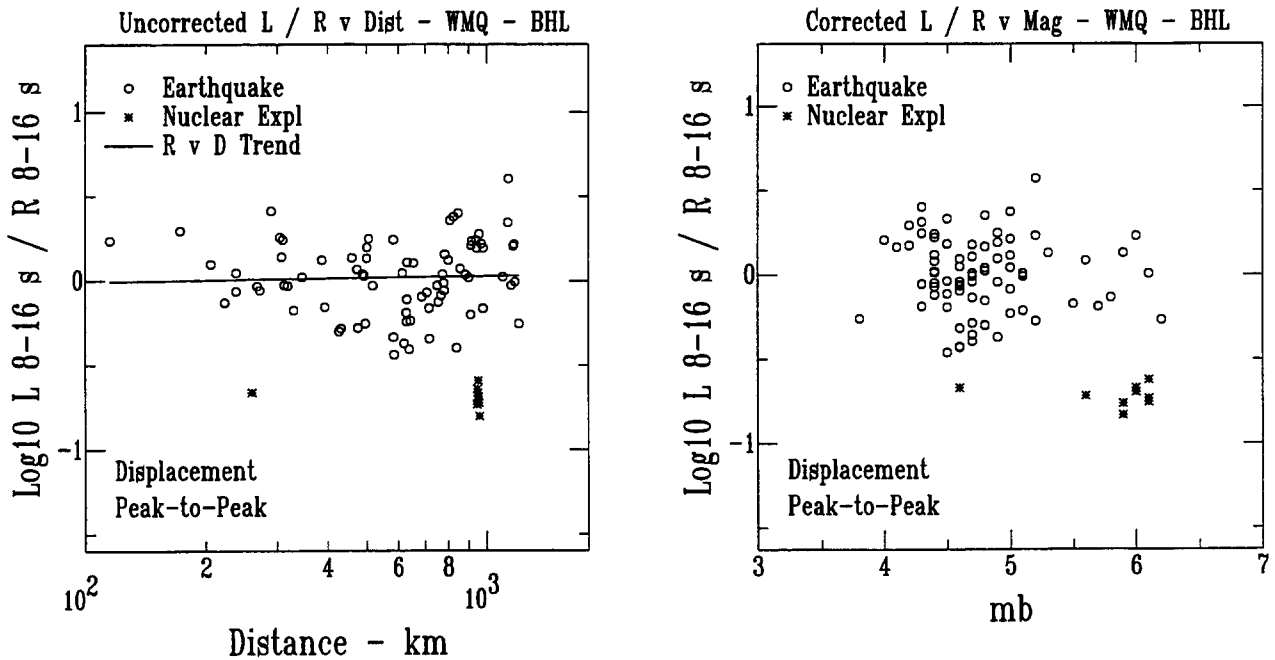


Figure 6. Long-period (8-16 s) discrimination plots for station WMQ. Rayleigh wave (R) is measured from vertical component, and Love wave (L) is measured from tangential component of broadband (BH) displacement records. Distance corrections have been applied to the ratio-magnitude plot as described under Figure 4. When Love-wave energy exceeds signal-to-noise levels, the L/R ratio is a viable discriminant.

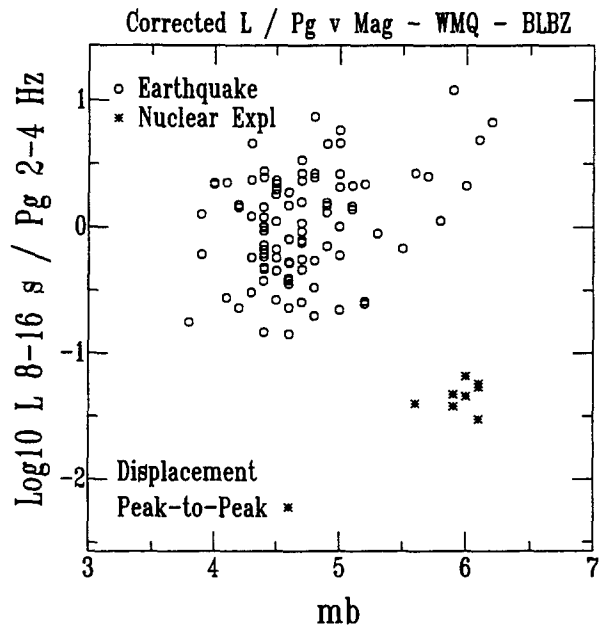
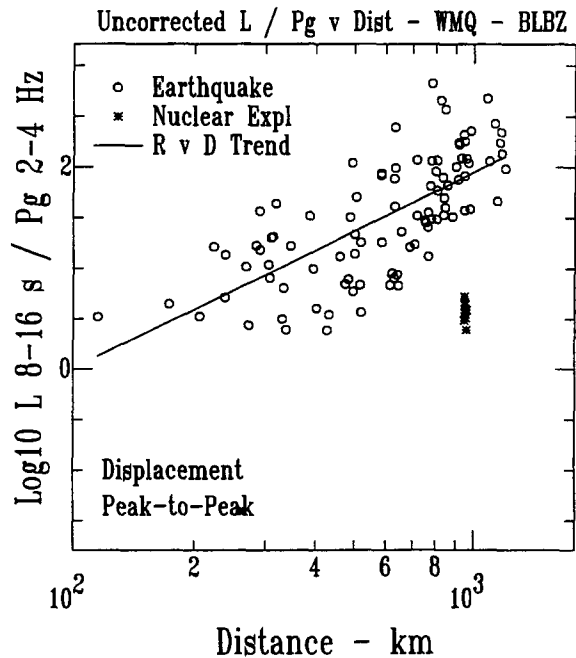
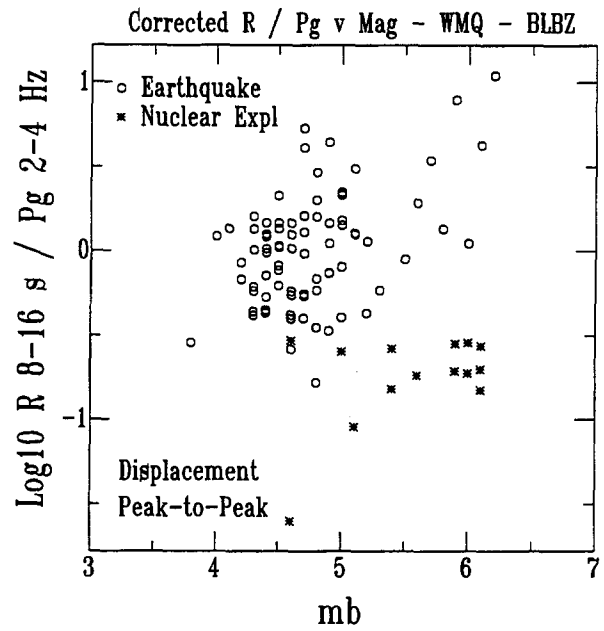
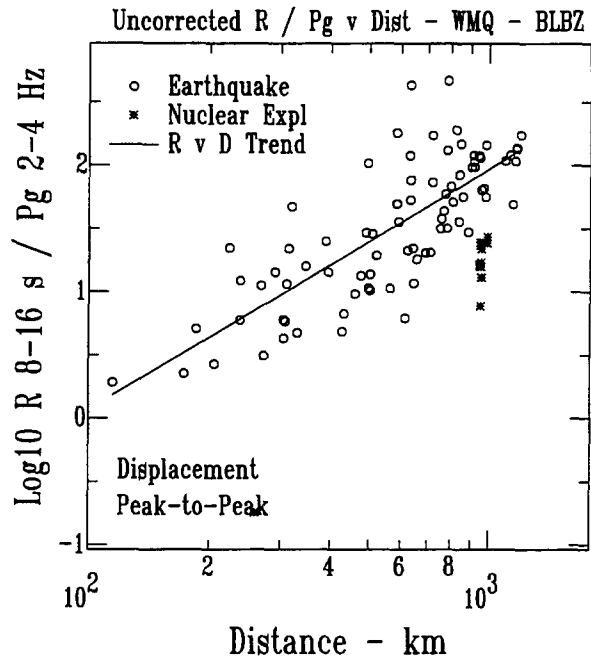
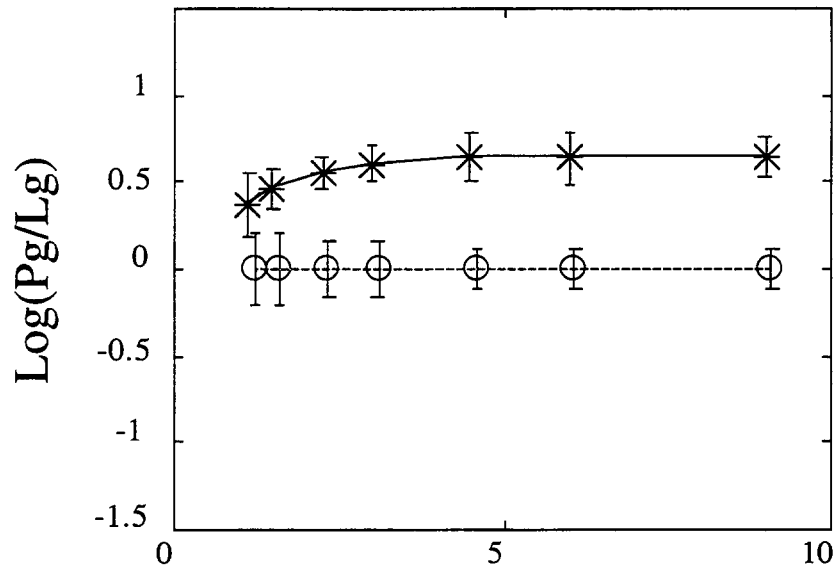


Figure 7. Long-period / short-period discrimination plots for station WMQ. *Top* shows $R(8-16s)/P_g(2-4Hz)$ results, and *bottom* shows $L(8-16s)/P_g(2-4Hz)$ results. Distance corrections have been applied to the ratio-magnitude plot as described under Figure 4. Waveform peak-to-peak amplitudes are measured from broadband (BH) displacement records.

Western China



Western U.S.

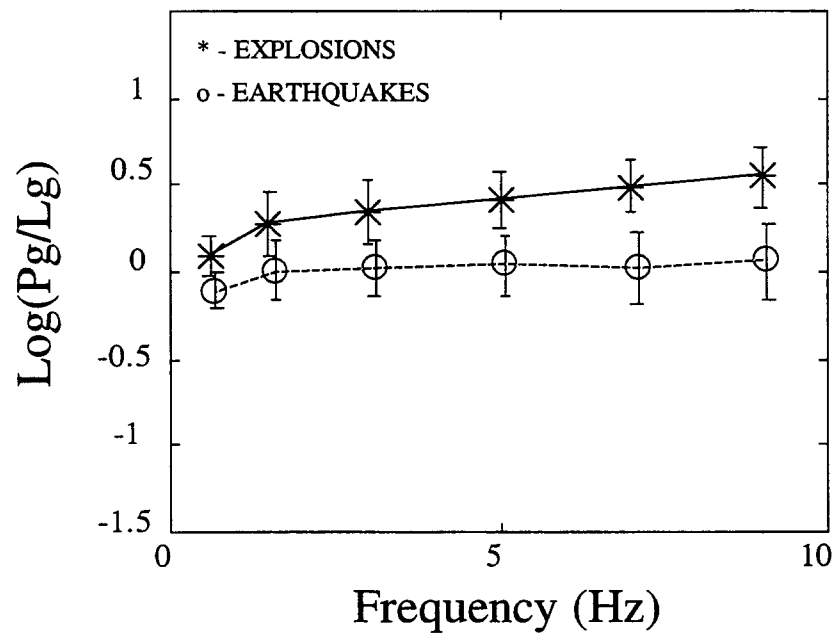


Figure 8. Short-period (P_g/L_g) ratio versus frequency for western China (*top*) and western United States (*bottom*). Circles show average ratios for earthquakes and asterisks show average ratios for nuclear explosions. Error bars are for 1 standard deviation. Above about 3 Hz separation between earthquakes and explosions for China is greater than for U.S. and scatter appears to be reduced.